Bulk and surface excitons in solid neon

V. Saile
Sektion Physik der Universität München, 8000 München 40, Federal Republic of Germany

E. E. Koch
Deutsches Elektronen-Synchrotron DESY, 2000 Hamburg 52, Federal Republic of Germany

(Received 27 November 1978)

Transmission and reflection spectra of solid neon in the valence-exciton range ($16 \leq h\nu \leq 22$ eV) have been carefully reinvestigated using highly monochromatized ($\Delta E = 4$ meV) synchrotron radiation. A surface-exciton state at $h\nu = 17.15$ eV located 210 meV below the $n = 1$ ($j = 3/2$) bulk exciton is observed and unambiguously identified. Energy positions of the bulk exciton states and line shapes as well as new and more precise values for derived quantities have been determined and are discussed in view of recent theoretical predictions. For the first time we are able to resolve the spin-orbit splitting of the $j = 3/2$ and $j = 1/2$ states and study the influence of exchange interaction. The value of 90 meV for the spin-orbit splitting is close to the gas-phase result. Within a quantum-defect approach we evaluate a new band gap of 21.58 eV for solid Ne.

I. INTRODUCTION

The onset of electronic absorption in rare-gas solids (RGS) is characterized by a number of sharp exciton bands. These excitonic spectra have attracted much interest from both theoreticians and experimentalists. RGS have frequently been regarded as prototype substances for insulators due to their simple electronic structure in the ground state with valence bands formed by the outermost closed p-shell electrons and the weak Van der Waals forces in the crystal. In spite of this key role there are still conflicting views as to how to describe the exciton states in these materials.

The excitation energies E_n of the exciton bands have been mainly described in terms of a hydrogenic Wannier-Mott exciton model[1] based on the effective-mass approximation (EMA) and expressed in the well-known form

$$E_n = E_G - B/n^2, \tag{1}$$

with E_G the gap energy, B the binding energy, and n the principal quantum number. The spin-orbit splitting of the initial states results in two Rydberg series. For the two $n=1$ excitons with radii smaller than or close to the nearest-neighbor distance, the approximations used in a simple Wannier-Mott exciton model are no longer justified. Attempts have been made to calculate these lowest excitation energies by introducing the so-called "central-cell corrections".[2] The most recent theories describe the lowest excitons by the following approaches:

(i) The lowest excitons can be considered as excitations intermediate between the Wannier-Mott and Frenkel-Peierls[3] descriptions. Taking into account the band structure and assuming a localization of electron and hole in the same unit cell, Andreoni *et al.*[4,5] applied an integral-equation method to calculate the energy positions, oscillator strengths and the longitudinal-transverse splittings of the first excitons in solid Ar,[4] and Ne.[5] The main drawback of this theory is its limitation to states with electron and hole confined to the same unit cell. An extension to states with $n \gtrsim 1$ seems to be complicated within an *ab initio* calculation.

(ii) Starting from the corresponding atomic transitions $2p^6 \rightarrow 2p^5 ns, ns'$ in Ne, Boursey *et al.*[6] calculated the $n=1$ excitons in solid Ne on the basis of the repulsive-potential curves of the molecular excited states. This theory works very well for the $n=1$ states, but is inadequate for the higher transitions.

(iii) Resca and Rodriguez[7] described the energy positions of the $n=1$ excitons for all four rare-gas solids within the framework of an integral-equation approach.[4,5] In this theory the excitation energy is adjusted to any desired value between the atomic value and the EMA result by a parameter ρ/ρ_{cc} with an effective exciton radius ρ and central-cell radius ρ_{cc}. Exploiting the close connection between rare-gas atoms and solids, Resca *et al.*[8] extended the concept of a quantum defect to the excitonic series. As in atomic theory, the space is divided into a sphere around the nucleus and the space outside. The wave functions inside the sphere are assumed to be nearly independent of the main quantum number n. By parametrizing the potential inside the atom with the help of the known atomic excitation energies, and introducing for the solid the screening of the Coulomb interaction outside the atom, Resca *et al.* obtained agree-

ment with the experimental values for the whole excitonic series for all rare-gas solids.[8] In this concept the unknown effective masses of the excitons serve as parameters. This description provides in a very natural way the transition from a Frenkel to a Wannier-Mott picture. On the other hand, this approach is semiempirical by exploiting the well-known atomic excitation energies, and it yields only energy levels; no oscillator strengths or longitudinal-transverse splittings. A quantum-defect theory in the described framework has been applied to solid Ne by Resta.[9]

With the recent observation of surface-exciton states in Ar, Kr, and Xe[10] and new structures in some of the bulk-exciton bands, a new challenge has been put forward to further investigate these states experimentally and describe the exciton states theoretically. Several models have been developed to interpret surface excitons in rare-gas solids:

(i) The energy shifts and splittings in environments with different symmetry have been treated by Wolff[11] starting from the corresponding atomic excitations. The calculated splittings for localized excitations at the surface of Ar and Kr compare favorably with the experimental results.[12]

(ii) In the same spirit, Chandrasekharan and Boursey[13] extended their picture, described above, to excitations in the (100) and (111) surface planes, and obtained good values for the excitation energies of surface excitons in all rare-gas solids.

(iii) Ueba and Ichimura[14] established conditions for the energies of surface excitons relative to the bulk states by a localized-pertubation method. In this approach the excitation energies as well as the Davydov splitting are determined by two quantities—the environmental-shift term and the exciton-transfer term. The application to Ar, Kr, and Xe,[15] resulted in smaller splittings of the excitation energies than the spin-orbit splitting of the initial states.[16]

Solid neon is in principle the simplest insulator, possessing the largest optically determined band gap (nearly 22 eV). The information about the exciton states obtained by optical absorption, reflection, and energy-loss spectroscopy has been reviewed by Sonntag.[17] Considering the presently available experimental data for solid Ne, two striking features have to be noted: (i) No spin-orbit splitting of the exciton series could be detected until now, in contrast to all other RGS, although Pudewill *et al.*[18] observed a shoulder in the reflection spectrum from thick ($d \geq 1000$ Å) films on the low-energy side of the intense $n=1$ exciton band separated by approximately 0.2 eV from the main peak. It was not clear, however, whether this splitting could be assigned to the spin-orbit splitting. (ii) Surface-exciton states have not yet been reported for solid Ne, in contrast to all other RGS.[10] The only hint for the existence of such a state came from photoemission-yield experiments,[19] which showed for thin films an extra emission at 17.1 eV, well below the $n=1$ bulk-exciton states. This emission was thought to be due possibly to excitation of adsorbed single Ne atoms or clusters decaying via energy transfer to the gold substrate, thus leading to an extra photoemission below threshold.[20]

Thus new experiments were required in order to assess the validity of the above-mentioned theoretical approaches, and to investigate the anomalies of the experimental data in more detail. A careful reinvestigation of the electronic structure also seemed rewarding in view of the increasing interest in the luminescence properties of solid Ne,[21] as well as its properties as a matrix in matrix-isolation spectroscopy.[22]

In the present paper we present and discuss a detailed experimental reinvestigation of the excitonic spectrum of solid Ne. Much more accurate data obtained by high-resolution transmission and reflection measurements enabled us to resolve the anomalies and to observe for the first time the surface-exciton states as well as the spin-orbit splitting of the bulk-exciton states. A preliminary presentation of the reflection data has been given in Ref. 23. As we will demonstrate, such spectra are difficult to interpret due to the strongly varying optical constants in the excitonic region. Moreover, accurate energy positions for strong transitions can be obtained from reflection data only via a Kramers-Kronig analysis. We therefore developed a consistent interpretation, especially in the range of the $n=1$ excitons on the basis of reflection *and* transmission measurements. It should be noted here that, although the very recent theoretical approaches[7-9] used the reflectance data from Ref. 23 without corrections, the general conclusions in these papers are not affected.

After a short description of the experimental arrangement (Sec. II), absorption and reflection spectra are presented for several film thicknesses (Sec. III). The spectra, derived parameters, and the consequences for our present understanding of the exciton states are discussed in Sec. IV.

II. EXPERIMENTAL PROCEDURE

Our transmission and reflection experiments have been performed at the Synchrotron Radiation Laboratory at the Deutsches Elektronen-Synchrotron storage ring DORIS. The apparatus consists of a high-resolution 3-m normal-incidence mono-

chromator,[24] an ultrahigh-vacuum experimental chamber (working pressure 5×10^{-10} Torr after baking) equipped with a He-flow cryostat, a reflectometer, and a gas handling system for sample preparation. For the solid-state experiments described here, we have chosen a medium wavelength resolution of 0.15 Å (≈4 meV at 18 eV) over the whole spectral range (300–3000 Å). We note that this resolution is about 30 times better than the half-width of the sharpest structure observed in the spectra. The instrument was calibrated by rare-gas absorption lines, and provides a reproducibility of 0.1 Å (2 meV at 17 eV). The neon samples were prepared by slow condensation of the sample gas (L'Air-Liquide, purity>99.995%) onto the cooled sample holder. The gas handling system was fully bakable and the purity of the Ne was checked with a mass spectrometer. For the transmission measurements, the Ne gas was condensed onto a LiF substrate coated with sodium salicylate for converting the vacuum-uv radiation transmitted through the sample into photons with λ roughly 4000 Å. This long-wavelength radiation was measured by a closed EMI 9804 photomultiplier. For the reflectance measurements, thin films were prepared in the same manner by condensing the gas on a gold-coated LiF crystal. For these measurements the angle of incidence was 7.5°. An open 20-stage electrostatic photomultiplier (Johnston MM2) served as a detector. One major drawback of this technique to measure transmission is its sensitivity to luminescent light emitted by the sample which cannot be distinguished from the transmitted light. On the other hand, with a solid angle of only 6×10^{-3} sr accepted by the open multiplier, luminescence does not play a role in our reflection geometry. By comparing the data sets measured with both techniques, we can estimate the influence of luminescence. It turned out to become important only for thick ($d\gg 100$ Å) samples.

The substrate temperatures for condensing the gas were varied between 6 and 9 K in order to test the influence of substrate temperature on the spectra. Although we observed slight changes in the spectral features, all conclusions drawn below are independent of temperature effects.

The measurements were performed with samples having different thicknesses in order to study also the influence of this parameter. In particular, it was possible in this way to discriminate roughly between surface and volume excitations. The thickness of the films could be determined in principle by observing the changes of the interference in the transparent part of the spectrum below the $n=1$ exciton with increasing film thickness during condensation. For Ne this method gave very poor results, since the refractive index is close to 1 in that range of the spectrum.[17] Furthermore, the technique employed in the transmission experiments using a comparatively rough sodium salicylate substrate prevented us from observing clear interferences. Thus we can only give estimates for the various film thicknesses.

A major consequence of this is the fact that we had to refrain in the present study from determining optical constants. We have plotted for the transmission experiments the optical density, that is, $-\ln[I(\omega)/I_0(\omega)]$, without correcting for the reflectance, where I and I_0 are the transmitted and incident intensities, respectively. Thus in the discussion of our results, the emphasis is on the excitation energies, on the relative intensities of various spectral features, and on the line shape of the exciton bands, while the optical constants could not be determined to an accuracy better than previously possible.[18]

III. RESULTS

A general view of the optical density of Ne recorded at a temperature of $T=6$ K appears in Fig. 1. Compared to previous results obtained with lower resolution,[18,25,26] a much more detailed structure in the excitonic region is clearly resolved in this spectrum. Furthermore, it is apparent that Ne is almost 100% transparent in the spectral region above and below the first exciton band. Spectra for the range of the $n=1$ excitons at around 17.5 eV are shown in more detail in Fig. 2 for a sequence of film thicknesses where $d_0<d_1<d_2<d_3<d_4$. For very thin films (d_0) we observe one single peak A centered at 16.91 eV. For this film thickness, no other absorption feature appears in the whole spectral range $16\leq h\nu\leq 22$ eV. We estimate the thickness d_0 to be equal to one monolayer or even less. Comparing the intensities, it is interesting

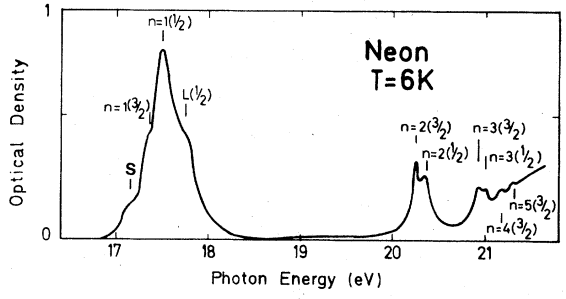

FIG. 1. Optical density $[-\ln(I/I_0)]$ of solid neon in the excitonic range of the spectrum. The main features can be grouped into two series split by spin-orbit interaction. See text for the assignment.

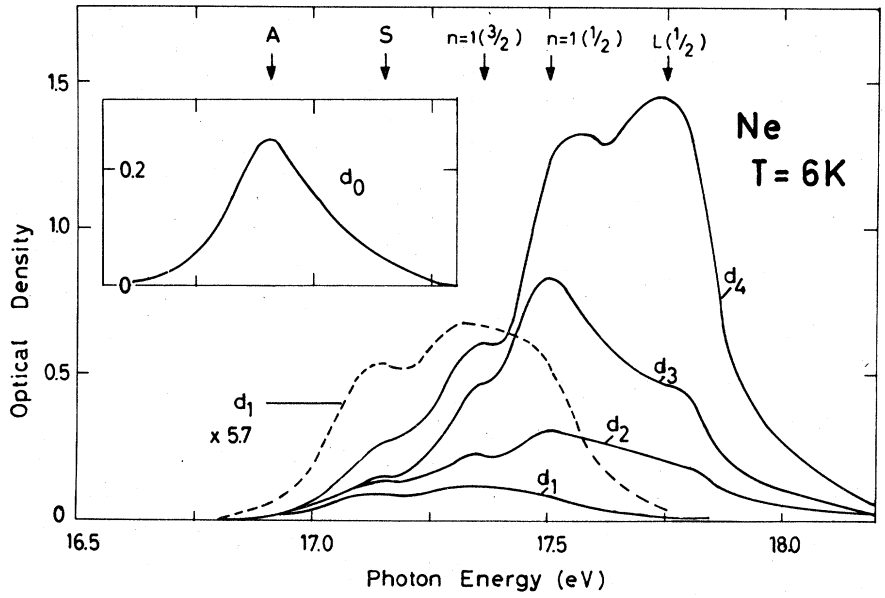

FIG. 2. Sequence of spectra $[-\ln(I/I_0)]$ for solid neon in the range of the first excitons for increasing film thicknesses d_0 (inset) to d_4. See text for the assignment of the various peaks or shoulders. Note that d_1–d_4 are different from the values denoted by the same symbols in the other figures.

to note that peak A is quite intense, e.g., with respect to the structure observed for d_1. When the thickness of the films is increased, peak A disappears and up to four features can clearly be discriminated. The peak at 17.15 eV, which we have denoted by S, is intense for thin films. For thicker samples, its intensity does not increase as rapidly as the maxima denoted by $n=1$ ($\frac{3}{2}$), $n=1$ ($\frac{1}{2}$) and L ($\frac{1}{2}$). The peak denoted by L appears first as a shoulder (d_2, d_3) and finally develops into a separate maximum for thicker samples.

Turning now to the reflectance data in the same spectral range (Fig. 3), we can identify the same four features in the spectrum obtained for the thickest sample (d_5). They appear almost at the same energies as in the absorption experiment. However, due to the high constant reflectance of the Au substrate and the weak Ne absorption outside the exciton bands, the situation is more complicated and one observes typical interferences for the vacuum–Ne-film–Au-substrate combination. Thus it is important to follow the changes of the spectra with increasing film thickness from d_1 to d_5 in order to identify the structures correctly. For example, there appears a typical interference minimum between 16.5 and 17 eV preceding the first exciton band. This minimum disappears almost completely for the thicker samples, whereas, e.g., the structure denoted by S persists for all thicknesses on a strongly varying background. It is also interesting to observe how the reflectance band between 17.5 and 18 eV develops into a broad stop band. Pudewill *et al.*[18] have measured for this band a reflectance of almost 60% for thick films with $d \approx 1000$ Å.

In Fig. 4 the optical density as well as reflectance spectra for a sequence of film thicknesses are displayed for the range $n>1$. The assignment of the bands is given at the bottom of the figure. Again it is possible to establish a one to one correspondence between the absorption maxima and the features of the reflectance spectra. As already noted by Pudewill *et al.*,[18] one observes a sort of trans-

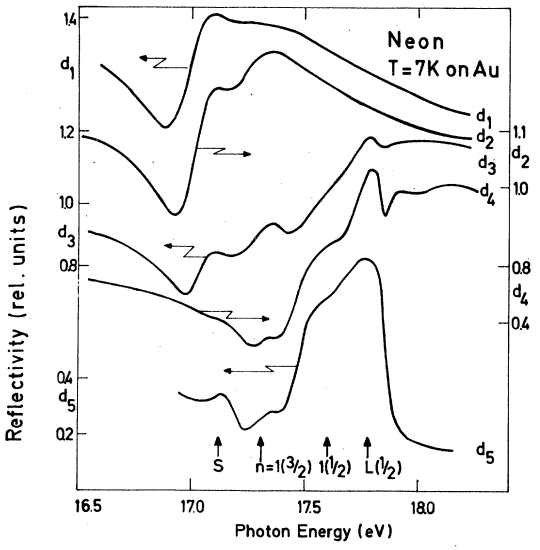

FIG. 3. Sequence of reflectance spectra of solid neon in the range of the first excitons for increasing film thicknesses d_1 to d_5. The assignment of the various features is the same as in Figs. 1 and 2 (see text). Note that d_1–d_4 are different from the values denoted in by same symbols in the other figures.

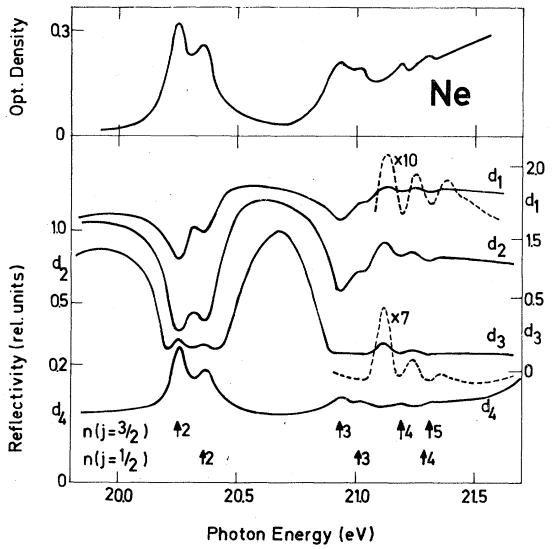

FIG. 4. Optical density $[-\ln(I/I_0)]$ of solid neon in the range of the higher excitons $n>1$ (upper part), and a sequence of reflectance spectra in the same range for increasing film thicknesses d_1 to d_4 (lower part). The assignment of the various features is the same as in Figs. 1–3 (see text). Note that d_1–d_4 are different from the values denoted by the same symbols in the other figures.

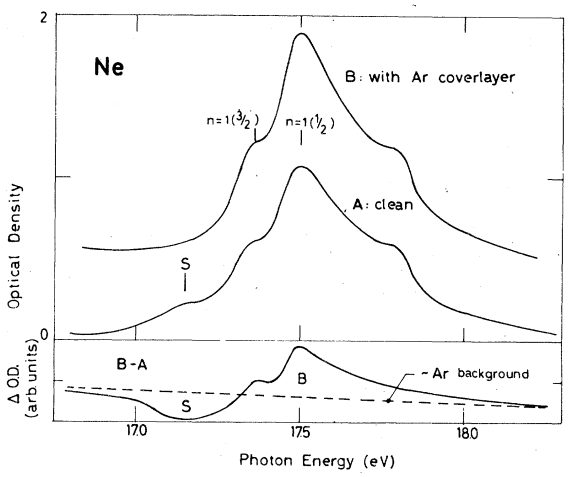

FIG. 5. Results for a surface-coverage experiment for solid neon in the range of the $n=1$ exciton. Curve A is the optical density $[-\ln(I/I_0)]$ of a clean neon sample. Upon evaporation of a thin Ar cover layer, the structure denoted by S disappears, whereas the band shape of the remaining peak remains unchanged. In the lower part, the different spectrum B-A is shown and the smooth and structureless Ar background is indicated by the broken line.

mission spectrum in a reflection geometry for thin Ne films on a highly reflecting substrate. The reflectance of the Au substrate is attenuated by weak transitions in the rare-gas film which are observed as dips in the reflectance spectrum (e.g., for d_1 and d_2). Our new data allow us to follow the changes with increasing absorption of light in the Ne film in detail. Thus, e.g., between d_2 and d_3 the dips turn into small peaks, until finally for d_4 fully developed reflectance bands are observed for the same energies. We note, however, that for d_4 strong contributions from the Ne-Au interface could be observed in the highly transparent region of Ne, i.e., below 17 eV (see Fig. 3) and between the $n=1$ and 2 excitons from about 18.3 to 19.8 eV.

Finally, in Fig. 5 the results of a surface-coverage experiment are presented. This experiment was performed in order to experimentally identify surface-exciton states. Curve A represents the optical density of a clean Ne sample in the range of the $n=1$ excitons. Curve B represents the optical density of the same Ne sample coated with a thin Ar film. The general background is increased since Ar has a smooth but non-negligible absorption in this region.[17] The most striking observation, however, is the disappearance of the structure S, while the other features remain essentially unchanged. The technique used here and the results and conclusions are similar to the observations for Xe, Kr, and Ar in previous experiments.[10] Together with the dependence of the absorption upon film thickness as discussed above, we take this finding as strong evidence for the fact that the additional maximum S is due to a surface exciton. The difference spectrum normalized to an almost constant Ar background absorption outside the Ne exciton bands shows that the intensity lost in the range of the surface exciton due to the cover layer is almost equal to the gain for the bulk excitons. Experiments with Xe and Kr cover layers gave essentially the same results. We further note that the disappearance of the surface peak can also be observed in the reflectance spectra, although due to additional interference effects with light reflected at the cover layer-Ne interface admittedly in not so clear a manner.[27]

IV. DISCUSSION

Several models for the exciton states in solid Ne have been discussed, and results of several recent calculations are available[5,6-9,13] in the literature. In the following we shall try to confront these predictions with the experimental results. A synopsis of the experimentally determined excitation energies appears in Table I, which also implicitly gives our assignments. The energies of the various exciton states are compared to atomic[28] $2p^6$

TABLE I. Energy positions of excitons in solid neon and derived quantities. All energies are given in eV. The accuracy is better than 0.01 eV for peak positions and 0.03 eV for the derived values unless otherwise noted in text. $E_G^{(1)}$ and $B^{(1)}$ are energy gaps and binding energies derived with the Wannier formula; $E_G^{(2)}$ and $B^{(2)}$ the same values after introducing a quantum defect δ. Δ_i are ths splittings between the $j=\frac{3}{2}$ and $\frac{1}{2}$ states. The value in column $E_G^{(1)}$ is the spin-orbit splitting of the Ne $2p$ levels. L-T is the longitudinal-transverse splitting. Transmission and reflection data are denoted by T and R, respectively, while G denotes values for gaseous Ne taken from Moore's tables (Ref. 28). The peak near 17.8 eV is ascribed to the excitation of a longitudinal exciton, which leads to the longitudinal-transverse splitting in the last row. The peak at 16.19 eV denoted by an asterisk is observed only for extremely thin films having thicknesses in the order of or below one monolayer. For $n=1$ ($j=\frac{1}{2}$) and L ($\frac{1}{2}$), a difference in energy positions between reflection and transmission is observed due to the high oscillator strength of that transition.

Wannier notation	n			1	2	3	4	5	$E_G^{(1)}$	$B^{(1)}$	$E_G^{(2)}$	$B^{(2)}$	δ
Surface exciton	T	16.91*	17.15										
	R		17.12										
	G	16.85											
$j=\frac{3}{2}$	T			17.36	20.25	20.94	21.19	21.32	21.50±0.03	5.00	21.58±0.03	6.93	0.28±0.03
	R			17.36	20.25	20.93	21.19	21.32					
	G			16.67	19.69	20.57	20.95	21.15	21.57		21.57		
$j=\frac{1}{2}$	T			17.50	20.36	21.02			21.58±0.04	4.90	21.62±0.06	6.32	0.24±0.03
	R			17.58	20.36	21.02	~21.29				21.64±0.06	6.67	0.28±0.03
	G			16.85	19.78	20.66	21.04	21.24	21.66		21.66		
Longitudinal exciton	T			~17.75									
	R			~17.78									
Δ_i	T			0.14	0.11	0.08			0.09				
	R			0.22	0.11	0.09	0.10						
	G			0.18	0.09	0.09	0.09	0.10	0.10				
L-T splitting	T			0.25									
	R			0.20									

$\rightarrow 2p^5ns, ns'$ transition energies involved with the lowest $2p^6$ electron excitation. In the following discussion we shall first deal with the adsorbate and surface excitations and then turn to the bulk exciton states.

A. Adsorbate state and surface excitons in solid neon

We assign the maximum A observed only for mono- or submonolayers of Ne to an adsorbate resonance. The excitation energy of 16.91 eV is close to the value for the $2p^6 \rightarrow 2p^5 3s, j=\frac{1}{2}$ state in the gas phase at 16.85 eV.[28,29] The disappearance of maximum A for thicker samples gives further evidence that the resonance is associated with excited states of adsorbed atoms or of small Ne clusters which exist prior to the formation of thin coherent Ne films.

The behavior of the surface-exciton state S observed at 17.15 eV in transmission and 17.12 eV in reflection is quite different in that it can be observed for the full sequence of film thicknesses. Evidence that this exciton state is confined to the Ne surface is based on the following observations: (i) The surface exciton is only observed under ultrahigh-vacuum conditions; (ii) upon coating with a different rare-gas film the surface exciton disappears (see Fig. 3); (iii) from the thickness dependence of the surface-exciton peak (Fig. 2), where the contribution of the surface exciton remains almost constant, whereas the bulk peaks increase with increasing film thickness, we estimate that the absorption due to surface excitons is confined to one layer at the sample-vacuum boundary. Such a localization has been experimentally demonstrated for the other RGS.[30]

For this new state in solid Ne introduced by the presence of the surface, we find a full width at half maximum (FWHM) of about 80–300 meV, depending on the sample preparation and background subtraction for deconvolution. These half-widths considerably exceed those for other RGS, where 20–30 meV have been observed.[10] Two different reasons can be responsible for such a broadening: Either the surface exciton is broadened by the same mechanism which causes a broadening of the bulk $n=1$ excitons in solid Ne compared to other

RGS (see below), or this surface peak consists of more than one overlapping excitation. As for the second argument, it has been shown both experimentally[10] and theoretically[11-13] that three transitions to surface states correspond to the two $n=1$ bulk excitons in RGS. We also expect three states below the $n=1$ ($\frac{3}{2}$) bulk exciton for Ne. From an extrapolation of the splittings of surface excitons in Ar and Kr (Ref. 10) to the case of Ne we estimate that they are confined to an energy interval of less than 200 meV. Chandrasekharan and Boursey recently calculated the excitation energies for surface excitons[13] in solid Ne on the basis of the molecular excited states derived from the first two atomic excitations and the Van der Waals interaction.[6] In this local picture, surface excitons are introduced by the different symmetries C_{4v} or C_{3v} compared to the bulk O_h symmetry. Their *ab initio* calculations yield three states at about 17.30 eV with a splitting of about 150 meV between the first and third peak. Taking into account a natural half-width of 80 meV ($\frac{1}{3}$ of the bulk widths as for the lighter rare-gas solids) for the surface excitons, this result is consistent with the experimental observation of one rather broad structure at 17.1 eV.

B. Bulk excitons

The excitation energies for the bulk excitons as well as derived parameters are collected in Table I. Our assignments for the bulk-exciton states have already been given in Figs. 1–5. Following previous studies,[18,25,26] we gave them in terms of the Wannier-Mott picture. For the first time two series are observed, and denoted by $\frac{3}{2}$ and $\frac{1}{2}$, and considerable improvements in the fine structure of the spectra and the accuracy of the data have been possible. Thus we are able to present a new consistent assignment for the observed transitions, and extract improved values for the derived quantities. Values for the band gaps E_G and binding energies B have been evaluated following the traditional concept of a least-squares fit for the experimental data $n\geq 2$ on the basis of the Wannier formula [Eq. (1)]. In this way we obtained the values $E_G = 21.50$ and 21.58 eV for the $j=\frac{3}{2}$ and $\frac{1}{2}$ series, respectively. It has been pointed out recently that this approach is inadequate for solid Ne.[8,9] Following Resca *et al.*[8] and Resta,[9] we introduced in Eq. (1) a quantum defect δ by replacing n^2 by $(n+\delta)^2$. Instead of two unknown quantities, E_G and B, we now deal with three, including δ. In principle δ is a function of the principal quantum number n,[31] but for a noninteracting series it is reasonable to assume a constant δ in a quantum-defect theory. This is corroborated by the numerical values obtained in Refs. 8 and 9 and by the theoretical analysis of the atomic data.[32] With three excitation energies for the excitons $n=1, 2$, and 3 we are able to extract by numerical methods the three values denoted by $E_G^{(2)}$, $B^{(2)}$, and δ in Table I. We note here that this method results in a good fit for all excitons, including the $n=1$ states. The introduction of a quantum defect overcomes the often discussed problems of a transition between Wannier-like excitations and Frenkel-type excitations with decreasing quantum number. At 21.58 eV, the band gap coincides with the ionization limit for the free atom. As for all these extrapolations, the accuracy is considerably lower than for the excitation energies involved. Furthermore, for the $j=\frac{1}{2}$ series we have only three states to determine three unknown quantities, and it is difficult to accurately extract the value for the $n=1$ ($\frac{1}{2}$) state: for transmission it is found at 17.50 eV for thin films and 17.53 eV for thick ones after deconvolution of the strongly overlapping L ($\frac{1}{2}$), $n=1$ ($\frac{1}{2}$), and $n=1$ ($\frac{3}{2}$) peaks. For reflection we obtained 17.58 eV for $n=1$ ($\frac{1}{2}$), but no Kramers-Kronig analysis has been performed to calculate the absorption maxima with these data. Due to these reasons, the reliability of $E_G(j=\frac{1}{2})$ is considered to be lower than that of $E_G(j=\frac{3}{2})$. Our value for the spin-orbit splitting of the Ne $2p$ states is therefore *not* the difference of the two gap energies, but rather the splitting of the $n=3$ excitons which are not affected by exchange interaction, as with the states with lower n (see Ref. 5). The value of 0.09 eV coincides, within the experimental error of 0.01 eV, with the splitting for the ionization limits $^2P_{3/2}$ and $^2P_{1/2}$ in the atom.[28] The extrapolated band gap of (21.58 ± 0.03) eV is slightly less than the 21.69 eV reported previously.[18] The most obvious influence of a quantum defect $\delta>0$ is found for the binding energies, which are increased by about 30%.

In Table II we compare our experimental results with recent theoretical predictions. There is generally good agreement between theory and experiment. Since the higher numbers of the series are rather well described in a hydrogeniclike picture for the spread out states, the good agreement for $n\geq 2$ is not surprising once the proper value for E_G has been obtained. This holds also for a quantum-defect theory as long as the quantum defect is small compared to 1. The tightly bound lowest $n=1$ levels are more difficult to describe, and pose more serious problems.

A complete theoretical analysis of the exciton states of solid neon has been presented by Andreoni *et al.*[5] For the $n=1$ exciton the main approximation was to assume that the electron and the hole are confined to the same unit cell (one-site approximation). This seems justified in view of the small

TABLE II. Comparison between experimental transition energies for bulk excitons in solid neon and other parameters with theoretical calculations. $B_1 = E_G - E(n=1)$ are the real binding energies of the $n=1$ excitons, Δ_{so} is the spin-orbit splitting and μ is the effective mass. The other notations are the same as in Table I. All energies are in eV.

	Experiment				Theory							
	Present work		Ref. 5		Ref. 6		Ref. 7		Ref. 8		Ref. 9[a]	
J	$\frac{3}{2}$	$\frac{1}{2}$	$\frac{3}{2}$	$\frac{1}{2}$	$\frac{3}{2}$	$\frac{1}{2}$	$\frac{3}{2}$	$\frac{1}{2}$	$\frac{3}{2}$	$\frac{1}{2}$	$\frac{3}{2}$	$\frac{1}{2}$
$n=1$	17.36	17.50			17.50	17.63	17.65	17.75	17.58	17.79	17.75	17.85
2	20.25	20.36	19.98	20.08					20.24	20.35	20.32	20.42
3	20.94	21.02	20.93	21.13					20.91	21.03	20.94	21.04
4	21.19	21.29	21.25	21.34					21.19	21.31	21.19	21.29
5	21.32		21.40	21.50					21.33	21.45	21.31	21.41
E_G	21.58	21.62	21.67	21.77					21.61	21.73	21.55	21.65
B_1	4.22	4.12	4.16	3.81								
Δ_{so}	0.09		0.10						0.12		0.10	
δ	0.28	0.24							~0.5		0.35	
μ	0.8	0.7	0.8						0.97		0.8	

[a] Gap energies are obtained by a fit of the experimental data, Ref. 23 (see also Ref. 27), and Δ_{so} is the atomic value. From these gap energies we subtracted the theoretical exciton binding energies.

Bohr radii of the $n=1$ excitons. The results based on the integral-equation approach including the band structure appear in Table II. While the theoretical results for the $n=1$ binding energies are in fair agreement with experiment, the calculated intensity ratio $I(n=1, \frac{3}{2}) : I(n=1, \frac{1}{2}) = 1:50$ is considerably smaller than the experimental one, for which we roughly estimate values between 1:5 and 1:10. If we apply our data to the theoretical dependence[5] of the intensity ratio and the splitting of the $n=1$ states (see Table I) on $\eta = 2(J+D)/\Delta$, where J, D, and Δ are the short- and long-range exchange terms and the spin-orbit splitting, respectively, we find for both the splitting of 0.14 eV and the ratio a value $\eta = 1.2-1.8$, while the calculations in Ref. 5 yield $\eta = 3.7$. For the states $n \geq 2$ Andreoni *et al.*[5] give an estimate for the excitation energies and intensity ratios based on the atomic values and the effective-mass approximation Eq. (1) with a given B and corrections for electron-hole exchange and spin-orbit splitting. Similarily as for the $n=1$ excitons, we observe in the experiment quite different intensity ratios: for the $n=2$ excitons we estimate an experimental ratio $I(n=2, \frac{3}{2}) : I(n=2, \frac{1}{2}) \geq 1.2$ (see Fig. 4). Instead of $\eta = 0.8$ (Fig. 5 in Ref. 5), we obtain experimentally a smaller exchange interaction $\eta = 0.4$. Obviously the exchange interaction is considerably overestimated in this theory. A similar observation has been found for solid Ar.[30] Exploiting *ab initio* calculations of the potential curves for the molecular ^3P and ^1P states of neon,[33] Boursey *et al.*[6] calculated the two $n=1$ exciton states in the solid. With a parameter-free calculation they obtained values which are only 140 meV higher in energy than those observed experimentally. Resca and Rodriguez[7] calculated the lowest-exciton states in the framework of the integral-equation approach. With simple trial wave functions which have the proper behavior for both the EMA and the atomic limit, and with a parameter for the extension of these envelope functions relative to the central-cell radii, they obtained a reasonable description for the transition from an atomic to an EMA picture for the $n=1$ excitons in Ne, Ar, Kr, and Xe.

Remarkable progress in describing the whole exciton series for all RGS has been made by a quantum-defect theory developed by Resta and Resca *et al.*[8,9] In this semiempirical approach the known atomic binding energies determine the potential inside the atoms in the solid, while outside a statically screened Coulomb potential is assumed. For the exciton the true electron mass is assumed inside the atom, and outside an effective mass. Thus the close analogy between Rydberg states in rare-gas atoms and excitons in rare-gas solids is directly exploited. The experimental quantum defect of 0.24–0.28 is somewhat smaller than the theoretical one of 0.35 in Ref. 8. These differences in δ are probably the reason why the theoretical excitation energies are too high at low quantum numbers. The atomic values for δ, approximately 0.7, are much higher than those for the solid. An extension of the quantum-defect approach to all RGS is found in Ref. 8. The theory is essentially the same as in Ref. 9, but for the fit of the experi-

mental data the effective mass μ is treated as a parameter, owing to the fact that an effective mass at the bottom of the conduction band is inappropriate for localized states.[8] We also compare in Table II the various effective masses with the experimental value

$$\mu=[B\ (\mathrm{eV})/13.606\ \mathrm{eV}]\epsilon_0^2$$

with $\epsilon_0=1.24$.

C. Line shape and longitudinal transverse splitting for the $n=1$ bulk excitons

The observed line shape for the $n=1$ excitons (Figs. 2 and 3) is quite complicated and we can only hope to extract qualitative information concerning this point. This complication of the spectrum is due to (i) the strong overlap of surface states with bulk excitons, (ii) the proximity of the $n=1$ $(\frac{3}{2})$ and $n=1$ $(\frac{1}{2})$ bulk states (see above), and (iii) the appearance of the feature L on the high-energy side of the band which we identify as the excitation of longitudinal-exciton states (see below). Nevertheless, large widths of the $n=1$ $(\frac{3}{2})$ and $n=1$ $(\frac{1}{2})$ peaks in Ne of the order of 200 meV are obtained after deconvolution of the peaks. This value has to be compared with the half-widths for the $n\geq 2$ exciton states (roughly 100 meV) and the line shape of exciton states in other RGS. For example, the line-shape analysis of bulk excitons of Ar, Kr, and Xe yields Lorentzians with half-widths ≤ 80 meV.[23] Thus according to Toyozawa's model,[34] the weak exciton-phonon scattering case is realized for these systems. In contrast to this the estimate of roughly 200 meV for the half-widths in solid Ne is in favor of localized-exciton states (strong-scattering case), where motional narrowing is not important. We note that the localized nature of the $n=1$ excitons in solid Ne is also in accord with the current view of exciton dynamics obtained from luminescence experiments.[21]

We interpret the maximum denoted by L $(\frac{1}{2})$ at 17.75 eV (Fig. 2) as the longitudinal (LO) $n=1$ $(\frac{1}{2})$ exciton which has its transverse counterpart (TO) at 17.50 eV. Due to the smaller oscillator strength of the $n=1$ $(\frac{3}{2})$ bulk state, the longitudinal-transverse splitting for this transition is expected to be only 4 meV. Bulk excitons in cubic crystals are split by the long-range dipole-dipole interaction into longitudinal (with $\vec{E}$ parallel to $\vec{k}$, where $\vec{E}$ is the electric field vector and $\vec{k}$ is the momentum of the exciton) and transverse ($\vec{E}$ perpendicular to $\vec{k}$) excitons.[35] The observation of the longitudinal bulk excitons is usually restricted to electron energy-loss spectroscopy where they show up as maxima in $\mathrm{Im}(-1/\epsilon)$. In fact, in such experiments performed for Ne, the energy-loss peak associated with the $n=1$ excitons has been observed at 17.74 and 17.75 eV.[36,37] In optical ($\vec{k}\approx 0$) normal-incidence transmission experiments, the longitudinal excitons normally do not couple to the incident transverse electromagnetic field. However, in reflection geometry[38] and for rough surfaces,[39] optical excitation of longitudinal modes becomes possible. The increase of the longitudinal peak with increasing film thickness (Fig. 2) is most probably due to an increased surface roughness for these films.

Our assignment of peak $L(\frac{1}{2})$ is supported by the electron-loss experiments mentioned above and by the observation of the broad "quasi"-stop band between 17.5 and 18.0 eV in the reflectance from thick films, which yields $h\nu_{\mathrm{To}}\approx 17.5$ eV and $h\nu_{\mathrm{Lo}}\approx 17.8$ eV. The numerical value which we deduce for the LO-TO splitting in solid Ne is in very good agreement with the values calculated by Andreoni *et al.*[5] and by Boursey *et al.*[13] (see Table III). For solid Ar and Kr, Andreoni *et al.*[40] proposed an explanation for the dip in the reflection stop band between the transverse longitudinal excitation in terms of spatial dispersion and a dead layer for bulk excitons at the surface. However, the existence of such a layer of some 10 Å is still an open question. We note in passing that we have studied the excitation of the longitudinal modes in more detail in transmission experiments at non-normal incidence for thin films of solid Kr.[41] In this case the situation is conceptually more favorable since the two $\frac{3}{2}$ and $\frac{1}{2}$ $n=1$ bulk-exciton states do not overlap and carry roughly the same oscillator strengths.

V. CONCLUSIONS

We briefly summarize the results obtained in the previous sections in order to draw some general conclusions:

(i) Results from improved optical-transmission and reflection experiments have been presented for thin films of solid Ne. These results are important in that they resolved the anomalies for Ne as compared to the other rare-gas solids.

(ii) Evidence of an adsorbate-induced resonance state close to the excitation energy of the corresponding gas-phase transition has been obtained. It would be rewarding to extend these experiments at submonolayer coverage under well-defined surface conditions in order to eventually follow the gradual transition from isolated Ne atoms to clusters and to bulk Ne films and relate the results to theoretical predictions.

(iii) Similarily as for Ar, Kr, and Xe, it was possible to detect and study surface-exciton states which are introduced by the presence of the surface and which are spatially confined to a region

TABLE III. Comparison between experimental and calculated energies for the longitudinal-transverse splitting for the $n=1$ excitons in solid neon.

	Experiment				Theory			
	Optical excitation [a]		Electron energy loss [b]		Ref. 5		Ref. 13	
j	$\frac{3}{2}$	$\frac{1}{2}$	$\frac{3}{2}$	$\frac{1}{2}$	$\frac{3}{2}$	$\frac{1}{2}$	$\frac{3}{2}$	$\frac{1}{2}$
$n=1$		0.25		0.25	0.004	0.232	0.236	0.252

[a] Present work.

[b] From electron-energy-loss experiments (Refs. 36, 37) taking the difference in peak positions from the maximum in the loss spectrum to the maximum of ϵ_2.

close to it.

(iv) Extensive information has been obtained for the bulk-exciton states which can be described optimally by a Rydberg series including a quantum defect which is lower than theoretically estimated. The derived parameters are only partly in agreement with theoretical predictions. It was possible to observe the doublet splitting in the exciton lines and to extract the spin-orbit splitting of the valence-band maxima at the Γ point in the Brillouin zone. Furthermore, the influence of electron-hole exchange interaction was compared with theoretical data.

(v) Finally, for the $n=1$ excitons the excitation of longitudinal modes has been observed in both transmission and reflection experiments, and the nature of these states was briefly discussed.

Thus we believe that with these results and the relation to recent theoretical approaches, which we discussed, a full understanding of the static properties of excitons in solid Ne is at hand. Further information related to clustering and film formation may come from experiments where the sample parameters can be varied in a controlled manner over a large range. Recent photoemission experiments from submonolayer rare-gas films reveal interesting extra peaks which are not accounted for in the bulk density of states.[42] Deeper insight into the nature of the exciton states may also come from investigations of high-resolution luminescence, where the various states discussed in the present paper can be selectively excited and differences of their decay mechanisms might further elucidate their dynamical properties.

ACKNOWLEDGMENTS

We are very grateful to Dr. W. Andreoni, Professor G. F. Bassani, and H. W. Wolff for useful discussions, and Dr. E. Boursey, Dr. V. Chandrasekharan, Professor Resca, and Professor Resta for providing copies of their papers prior to publication. We are also particularly grateful to Professor W. Steinmann for his continuous interest and support of this project. This work has been supported in part by Bundesministerium für Forschung und Technologie BMFT from funds for Synchrotron Radiation Research.

[1] R. S. Knox, *Theory of Excitons* (Academic, New York, 1963).

[2] J. Hermanson, Phys. Rev. 150, 660 (1966); J. Hermanson and J. C. Phillips, *ibid.* 150, 652 (1966); U. Rössler and O. Schütz, Phys. Status Solidi B 56, 483 (1973).

[3] A. S. Davydov, *Theory of Molecular Excitons* (McGraw-Hill, New York, 1962).

[4] W. Andreoni, M. Altarelli, and F. Bassani, Phys. Rev. B 11, 2352 (1975).

[5] W. Andreoni, F. Perrot, and F. Bassani, Phys. Rev. B 14, 3589 (1976).

[6] E. Boursey, M.-C. Castex, and V. Chandrasekharan, Phys. Rev. B 16, 2858 (1977).

[7] L. Resca and S. Rodriguez, Phys. Rev. B 17, 3334 (1978).

[8] L. Resca, R. Resta, and S. Rodriguez, Solid State Commun. 26, 849 (1978); Phys. Rev. B 18, 696 (1978).

[9] R. Resta, Phys. Status Solidi B 86, 627 (1978).

[10] V. Saile, M. Skibowski, W. Steinmann, P. Gürtler, E. E. Koch, and A. Kozevnikov, Phys. Rev. Lett. 37, 305 (1976).

[11] H. W. Wolff, in *Extended Abstracts, Fifth International Conference on Vacuum Ultraviolet Radiation Physics, Montpellier*, edited by M. C. Castex, M. Pouey, and N. Pouey (CNRS, Meudon, 1977), Vol. I, p. 214.

[12] V. Saile and H. W. Wolff, in *Proceedings of the Seventh International Vacuum Conference and Third International Conference on Solid Surfaces*(R. Dobrozemsky, F. Rüdenauer, F. P. Viehböck, and A. Breth (Vienna, 1977),Vol. I, p. 391.

[13] V. Chandrasekharan and E. Boursey (unpublished).

[14] H. Ueba and S. Ichimura, J. Phys. Soc. Jpn. 41, 1974 (1976).

[15] H. Ueba, J. Phys. Soc. Jpn. 43, 353 (1977).

[16]We want to note here that H. Ueba apparently misinterpreted Ref. 10. Instead of two spin-orbit split-bulk excitons, three states at the surface for Ar and Kr had been observed in Ref. 10. Spin-orbit interaction is clearly present but is unable to explain the additional splitting of the $j=\frac{3}{2}$ excitation at the surface.
[17]B. Sonntag, in *Rare Gas Solids*, edited by M. L. Klein and J. A. Venables (Academic, New York, 1977), Vol. II, p. 1021.
[18]D. Pudewill, F.-J. Himpsel, V. Saile, N. Schwentner, M. Skibowski, and E. E. Koch, Phys. Status Solidi B 74, 485 (1976).
[19]E. E. Koch, V. Saile, N. Schwentner, and M. Skibowski, Chem. Phys. Lett. 28, 562 (1974).
[20]For a discussion of the processes involved see, e.g., D. Pudewill, F.-J. Himpsel, V. Saile, N. Schwentner, M. Skibowski, E. E. Koch, and J. Jortner, J. Chem. Phys. 65, 5226 (1976).
[21]See, e.g., G. Zimmerer, in *Luminescence of Inorganic Solids*, edited by B. Di Bartolo (Plenum, New York, 1978), p. 627.
[22]See, e.g., B. Meyer, Ber. Bunsenges. Phys. Chem. 82, 24 (1978), and references therein.
[23]V. Saile, W. Steinmann, and E. E. Koch, *Extended Abstracts of the Fifth International Conference on Vacuum Ultraviolet Radiation Physics, Montpellier*, edited by M. C. Castex, M. Pouey, and N. Pouey (CNRS, Meudon, 1977), Vol. I, p. 199.
[24]V. Saile, P. Gürtler, E. E. Koch, A. Kozevnikov, M. Skibowski, and W. Steinmann, Appl. Opt. 15, 2559 (1976).
[25]R. Haensel, G. Keitel, E. E. Koch, N. Kosuch, and M. Skibowski, Phys. Rev. Lett. 25, 1281 (1970).
[26]E. Boursey, J. Y. Roncin, and M. Damany, Phys. Rev. Lett. 25, 1279 (1970).
[27]These interference effects suppressed the weak $n=1$ ($\frac{3}{2}$) bulk state (d_5 in Fig. 3). Thus on the basis of reflection spectra only, we first tended to interpret this excitation as a surface exciton with, as a consequence, a different assignment for the $n=1$ ($\frac{1}{2}$) and L ($\frac{1}{2}$) states. Furthermore, this interpretation in Ref. 23 was consistent with that of Ref. 18.
[28]C. E. Moore, Natl. Bur. Stand. (U.S.), Circ. No. 467, 1, 76 (1949).
[29]We associate the adsorbate resonance with the $j=\frac{1}{2}$ state in the gas phase, whose oscillator strength is about 10 times that of the $j=\frac{3}{2}$ state [W. C. Wiese, M. W. Smith, and B. M. Glennan, *Atomic Transition Probabilities*, U. S. Natl. Stand. Ref. Data Ser. No. 4 (U.S. GPO, Washington, D.C., 1966), Vol. 1, p. 128].
[30]V. Saile, Thesis (Universität München, 1976) (unpublished).
[31]U. Fano, J. Opt. Soc. Am. 65, 979 (1975).
[32]A. F. Starace, J. Phys. B 6, 76 (1973).
[33]J. S. Cohen and B. Schneider, J. Chem. Phys. 61, 3230 (1974); 61, 3240 (1974).
[34]Y. Toyozawa, in *Vacuum Ultraviolet Radiation Physics*, edited by E. E. Koch, R. Haensel, and C. Kunz (Pergamon/Vieweg, Braunschweig, 1974), p. 317.
[35]W. R. Heller and A. Marcus, Phys. Rev. 84, 809 (1951).
[36]J. Daniels and P. Krüger, Phys. Status Solidi B 43, 659 (1971).
[37]L. Schmidt, Phys. Lett. A 36, 87 (1971); Thesis (Technische Universität Berlin, 1972) (unpublished).
[38]Analogous to the coupling of light to phonons as described, e.g., by M. Balkanski, in *Optical Properties of Solids*, edited by F. Abeles (North-Holland, Amsterdam, 1972), p. 529.
[39]I. Filinski, Phys. Status Solidi B 49, 577 (1972).
[40]W. Andreoni, M. De Crescenzi, and E. Tosatti, Solid State Commun. 26, 425 (1978).
[41]V. Saile and E. E. Koch (unpublished).
[42]K. Horn, M. Scheffler, and A. M. Bradshaw, Phys. Rev. Lett. 41, 822 (1978).